Scramjet Isolators

Professor Michael K. Smart
Chair of Hypersonic Propulsion
Centre for Hypersonics
The University of Queensland
Brisbane 4072
AUSTRALIA

m.smart@uq.edu.au

ABSTRACT

Scramjet operation in the lower hypersonic regime between Mach 4 and 8 is characterized by what is called dual-mode combustion. In this situation disturbances generated by heat-release in the combustor can propagate upstream of fuel injection to affect the operation of the inlet. The method use to alleviate this problem is installation of a short duct between the inlet and the combustor known as an isolator. This article describes the flow phenomenon that exits in the isolator in these situations and presents some of the current methodologies and analysis techniques for scramjet isolator design.

NOMENCLATURE

A	area (m^2)
c_p	specific heat (J/kgK)
C_f	skin friction coefficient
D	hydraulic diameter (m)
f_{st}	stoichiometric ratio
F	stream thrust (N)
h_{pr}	heat of combustion (J/kg of fuel)
H_t	total enthalpy (0K basis) (J/kg)
M	Mach number
P	pressure (Pa)
Q	heat loss to the structure (J/kg)
R	gas constant (J/kgK)
Re	Reynolds number
s	shock train length (m)
T	temperature (K)
V	velocity (m/s)
x	axial distance (m)
ϕ	equivalence ratio
ϑ	constant in mixing curve
γ	ratio of specific heats
θ	boundary layer momentum thickness (m)
η_c	combustion efficiency
ρ	density (kg/m^3)
τ	shear stress (Pa)

Subscript

c	core flow
t	total
w	wall

1.0 INTRODUCTION

Scramjet operation in the lower hypersonic regime between Mach 4 and 8 is characterized by what is called dual-mode combustion. Figure 1 shows a schematic of a scramjet powered vehicle operating in this way. In this instance, flow is compressed by shock waves in the forebody and inlet, and is supplied to the

combustor at supersonic conditions. Combustion of fuel with the incoming air generates a large local pressure rise and separation of the boundary layer on the surfaces of the combustor duct. This separation, which can feed upstream of the point of fuel injection, acts to further compress the core flow by generating a series of shock waves known as a shock-train. A short length of duct, called the isolator, is usually added to the scramjet flowpath upstream of the combustor to contain this phenomenon and stop it from disrupting the operation of the inlet. In some engines, the combination of diffusion in the isolator and heat release in the combustor decelerates the core flow to subsonic conditions. In this instance the core flow must then re-accelerate through Mach 1 in what is known as a thermal throat.

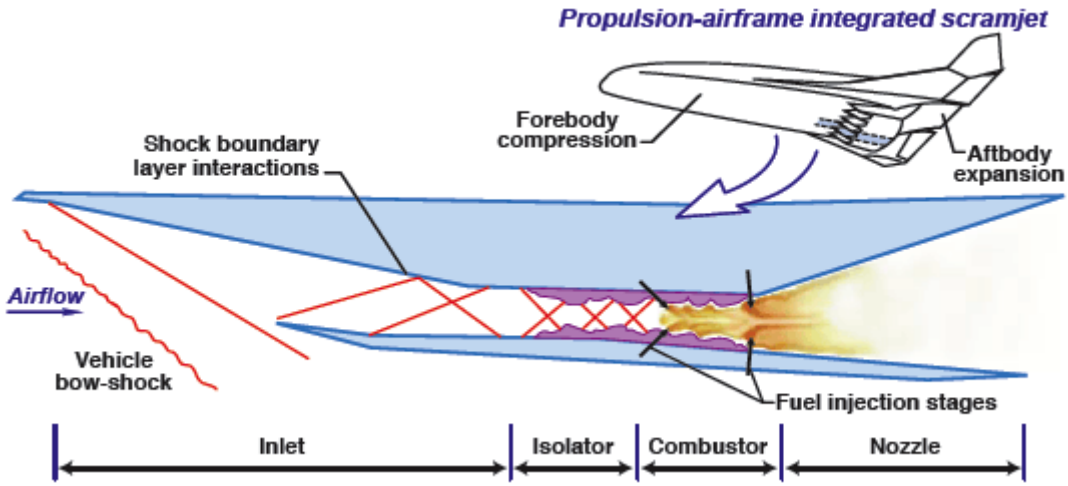

Figure 1: Schematic of a scramjet operating in dual-mode (NASA).

Dual-mode combustion can produce large pressure levels in the combustor and nozzle, generating high levels of thrust. This flow is affected by many parameters, including the state of the boundary layer in the isolator, the flow Mach number exiting the inlet, the area distribution of the combustor, and the position and number of fuel injection stations. As the separated regions on the surfaces of the isolator and combustor are seen by the core flow as blockage, scramjet engines operating in dual-mode can be thought of involving fluid-dynamic variable geometry. At speeds above Mach 8, the increased kinetic energy of the airflow through the engine means that the combustion generated pressure rise is not strong enough to cause boundary layer separation. Flow remains attached and supersonic throughout in the instance, and the engine operates as a pure scramjet.

The article will first describe the flow structure that occurs in the isolator of a dual-mode scramjet. Next, a diffuser model applicable to the analysis of dual-mode scramjet combustion will be presented. Some results of the analysis will then be compared to experiments.

2.0 FLOW STRUCTURE IN A SCRAMJET ISOLATOR

The structure of the supersonic flow in confined ducts under the influence of a strong adverse pressure gradient is of interest in the design of scramjet isolators. As shown in the schematic of Fig. 2, the pressure gradient is imposed on the incoming supersonic flow in the form of shock waves. If there were no boundary layer, a normal would form in a plane. However, the presence of an incoming boundary layer produces a series of normal or oblique shocks that can spread the pressure rise over a length of many duct diameters. This phenomenon, known as a “pseudo shock”[1] or “shock-train” is characterized by a region of separated flow next to the wall, together with a supersonic core that experiences a pressure gradient due to

the area restriction of the separation, forming a series of crossing oblique shocks in the core flow. A mixing region also grows between the core and separated flows, balancing the pressure rise in the core against the shear stress on the boundary of the separation. Finally, the flow reattaches at some point and mixes out to conditions that match the imposed back-pressure. Being able to predict the length scale of this flow structure is the key component of isolator design for dual-mode scramjets.

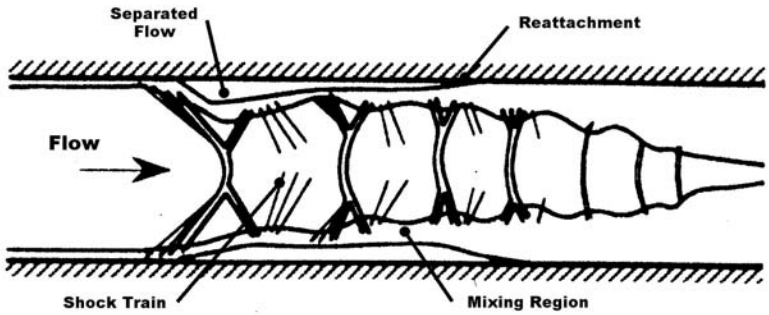

Figure 2: Schematic of flow structure in an isolator.

Important work on this phenomenon was performed by McLafferty[2] in the 1950's and by Waltrup and Billig[3] in the early 1970's. In this research it was observed that for a given imposed pressure rise (ΔP/P), the length over which the shock train spread varied with $D^{1/2}\theta^{1/2}$ and inversely with $(M^2 - 1)(Re_\theta)^{1/4}$, where D is the duct diameter, M is the Mach number of the inflow, θ is the momentum thickness of the boundary layer and Re_θ is the Reynolds number based on momentum thickness. Based on experiments in round ducts with incoming Mach numbers between 1.5 and 2.7, Waltup and Billig found that thicker boundary layers lead to longer shock trains,and developed the following empirical correlation for s, the distance over which the shock structure (or pressure rise) is spread:

$$\frac{s(M^2-1)(\mathrm{Re}_\theta)^{1/4}}{D^{1/2}\theta^{1/2}} = 50\left[\frac{\Delta P}{P}\right] + 170\left[\frac{\Delta P}{P}\right]^2 \qquad (1)$$

Figure 3 below, taken from Ref. 3, shows the form of the simple quadratic correlation in ΔP/P in comparison to the data used to develop the correlation.

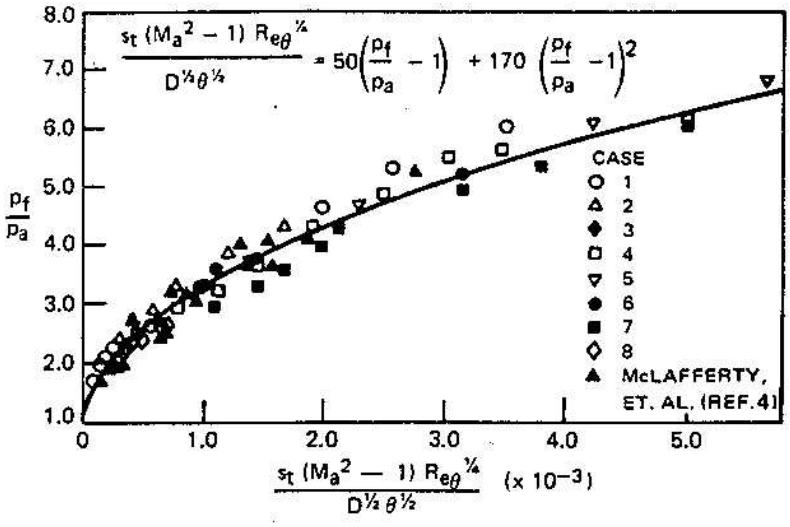

Figure 3: Correlation of experimental shock train data[3].

It has been postulated by many authors that the pressure gradient experience by the core flow in the duct must be equal to the pressure gradient that can be supported by shear in the separated region. Based on a large amount of experimental data at different Mach numbers, Reynolds numbers and in different duct geometries, Ortwerth[4] determined that the rate of pressure rise (diffusion) in a duct is directly proportional to the dynamic pressure of the incoming flow and the skin friction coefficient at the initial point of separation in the duct, and inversely proportional to the duct hydraulic diameter. From this he developed a diffuser model for separated flow in ducts which can be expressed as:

$$\frac{dP}{dx} \approx \frac{89}{D_H} C_{f0} \left(\frac{\rho V^2}{2}\right) \tag{2}$$

where D_H is the hydraulic diameter of the duct, C_{f0} is the friction coefficient at the initial separation point. In essence, this relationship supplies the ability to determine a length scale over which pressure rise must be spread in a duct. It will be used in the next section of this paper as the extra equation needed to perform quasi-one-dimensional calculations of flow properties in separated ducts.

3.0 DIFFUSER MODEL FOR SCRAMJET ISOLATOR FLOW ANALYSIS

Analysis of the combustion process in a scramjet usually involves quasi-one-dimensional cycle analysis methods. While the real combusting flow in a scramjet is far from uniform at any cross-section throughout the engine, when used properly, these techniques provide an efficient means of modeling isolator and combustor region of a scramjet. While some methods simply jump from the start to the end of the combusting zone[5], the method presented in this article enables prediction of the pressure distribution in the entire region of the engine affected by combustion, therefore enabling comparison with experimental pressure measurements. These methods follow directly from the classical quasi-one-dimensional gasdynamics presented by Shapiro[6], with the addition of Ortwerth's diffuser model to close the equation set.

A differential element of the separated flow in a duct is shown in Fig. 4. Here the area of the core flow passing through the duct (A_c), is equal to the geometric area of the duct (A) if flow is attached, but is less

than A for separated flow. Fuel and air are burning in this element, and a friction force $dFr = \tau_w A_w$ is applied by the walls, together with a heat loss in the amount dQ. For simplicity of analysis, the flow is assumed to be that of a calorically perfect gas with constant ratio of specific heats, γ, gas constant R, and specific heat at constant pressure, c_p. Combustion heat release is modeled through the use of a heat of combustion, h_{pr}, and the change in total enthalpy of the flow as it traverses the element is:

$$dH_t = h_{pr} f_{st} d\phi - dQ \tag{3}$$

where f_{st} is the stoichiometric fraction of fuel to air, and $d\phi$ is the equivalence ratio of fuel that combusts in length dx. The corresponding change in the total temperature of the flow is therefore $dT_t = dH_t/c_p$. The wall shear stress is related to a skin friction coefficient through $\tau_w = C_f \rho V^2/2$, and $A_w = 4Adx/D$, where D is the hydraulic diameter of the duct.

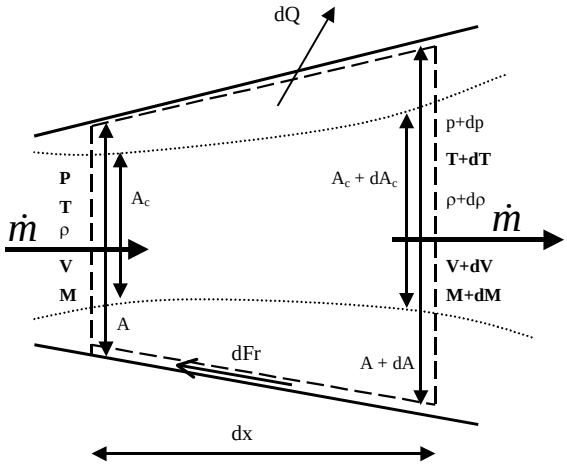

Figure 4: Differential element of separated flow.

The differential conservation equations of mass, momentum and energy for the element, are given by:

$$\frac{d\rho}{\rho} + \frac{dV}{V} + \frac{dA_c}{A_c} = 0 \tag{4}$$

$$\frac{dp}{p} + \frac{\gamma M^2}{2}\frac{4C_f dx}{D} + \frac{\gamma M^2}{2}\frac{A_c}{A}\frac{dV^2}{V^2} = 0 \tag{5}$$

$$\frac{dT}{T} + \frac{\gamma - 1}{2} M^2 \frac{dV^2}{V^2} = \left(1 + \frac{\gamma - 1}{2} M^2\right)\frac{dT_t}{T_t} \tag{6}$$

Note that these equations all apply to the core flow area, but friction and heat loss are based on the geometric area. Together with the equation of state for the gas and the definition of Mach number (in differential form):

$$\frac{dp}{p} - \frac{d\rho}{\rho} - \frac{dT}{T} = 0 \tag{7}$$

$$\frac{dM^2}{M^2} - \frac{dV^2}{V^2} + \frac{dT}{T} = 0 \tag{8}$$

we have five equations to relate the eight variables. Following Shapiro[6], area change (dA/A) and total temperature change (dT_t/T_t) are treated as independent variables. If the flow is attached, this closes the equation set and all 1-D axial property distributions in the duct can be calculated as described by the influence coefficients of Shapiro. For separated flows, however, an extra equation is needed for the extra variable, A_c. This is supplied by Ortwerth's diffuser relation (eqn 2). After a significant amount of algebraic manipulation of equations 2,4-7, the following differential relation for Mach number is obtained:

$$\frac{d(M^2)}{M^2} = -\left(1 + \frac{\gamma - 1}{2} M^2\right) \left[\frac{dp/p}{\frac{\gamma M^2}{2} \frac{A_c}{A}} + \frac{4C_f \frac{dx}{D}}{\frac{A_c}{A}} + \frac{dT_t}{T_t} \right] \tag{9}$$

This related the change in Mach number to the amount of diffusion (dP/P), the amount of heat release (dT_t/T_t), and the axial distribution of C_f. This must be integrated in conjunction with the following relation for A_c/A:

$$\frac{d(A_c/A)}{A_c/A} = \left[\frac{1 - M^2\left\{1 - \gamma\left(1 - A_c/A\right)\right\}}{\gamma M^2 A_c/A} \right] \frac{dp}{p} + \left(\frac{1 + (\gamma - 1) M^2}{2 A_c/A} \right) 4C_f \frac{dx}{D} + \left(1 + \frac{\gamma - 1}{2} M^2\right) \frac{dT_t}{T_t} \tag{10}$$

To determine the axial distributions of Mach number and A_c/A in ducts with specified area A(x) and prior knowledge of the heat release distribution, $T_t(x)$ and C_f, these equations can be integrated with a standard ODE solver for multiple equations.

This methodology will now be applied to a scramjet vehicle flying at Mach 7 and a dynamic pressure of 50 kPa. In keeping with the notation of Heiser and Pratt[7], station 0 is in the freestream flow ahead of the vehicle, and a streamtube with area A_0 is captured and processed by the engine. Station 1 is downstream of the vehicle forebody shock and represents the properties of the flow that enters the inlet. Station 2 is at the inlet throat, which is usually the minimum area of the flowpath, and the length between stations 2 and 3 is referred to as the isolator. Station 3 represents the start of the combustor, and fuel and air is mixed and burned by the end of the combustor at station 4. The nozzle includes an internal expansion up to station 9, and an external expansion to station 10 at the end of the vehicle.

Assuming a fairly typical forebody/inlet compression, the properties at the inlet throat (station 2) will be assumed to be $M_2 = 3.60$, $p_2 = 50$ kPa, $T_2 = 650$ K, $H_{t2} = 2.35$ MJ/kg. The axial distribution of properties in a round isolator/combustor duct with an initial diameter of 0.06m and a divergence with area ratio of 2 will be calculated for different fuelling levels. The start of the isolator is assumed to be at $x_2 = 0.0$ m, and hydrogen fuel ($h_{pr} = 120$ M/kg) is injected at $x_3 = 0.2$ m (the start of the combustor). The amount of fuel that is allowed to react with the air at a particular station is dictated by a mixing efficiency curve, $\eta_c(X)$, that takes the form:

$$\eta_c = \eta_{c,tot} \left[\frac{\vartheta X}{1 + (\vartheta - 1) X} \right] \tag{11}$$

where $\eta_{c,tot}$ is the combustion efficiency at the end of the combustor, X = (x-x3)/(x4-x3) and ϑ is an empirical constant of order 1 to 10 which depends on the rate of mixing[7]. For the current study $\eta_{c,tot}$ was

set to 0.8 at all times and a value of $\vartheta = 5.0$ was used. These values correspond to robust combustion in the engine. Making use of eqn. 11, the heat release curve is therefore:

$$T_t = T_{t2} + \left(h_{pr} f_{st} \phi \eta_c - dQ \right) / c_p \tag{12}$$

Skin friction was calculated assuming a constant skin friction coefficient of $C_f = 0.002$ and heat loss to the structure (dQ) was calculated using Reynolds analogy and an assumed wall temperature of $T_w = 600$ K.

Given the limitation of constant γ, R and c_p in the analysis, eqns. 9 and 10 are integrated in sections along the duct. In the isolator section upstream of fuel injection, values of $\gamma = 1.37$, R = 287 J/kg/K and c_p = 1063 J/kg/K were used. In the combustor, average values of $\gamma = 1.31$, R = 297 J/kg/K and c_p = 1255 J/kg/K were used, so as to model the properties of the real fuel/air/combustion products mixture which vary along the length of the combustor.

Figure 5 shows calculated 1-D flow properties in the duct for fuelling at an equivalence ratio of $\phi = 0.5$. In the isolator section of the duct the Mach number reduces and the pressure and temperature increase due to the action of friction on the duct surfaces. At the start of the combustor, flow properties are recalculated to be consistent with the values of γ and R used in the combustor integration, while conserving fluxes of mass, momentum and total enthalpy across the boundary between the isolator and combustor. Fuel is also added, and combustion along the duct leads to a drop in the Mach number, an increase in the temperature, and the pressure varies smoothly in response to the competing effects of combustion and area increase. The peak pressure and temperature in the duct are $P/P_2 = 2.19$ and $T/T_2 = 2.61$, and the minimum Mach number is M = 1.48. The analysis results in an estimate of the one-dimensional supersonic properties of the flow as it exits the combustor at $x_4 = 0.5$ m.

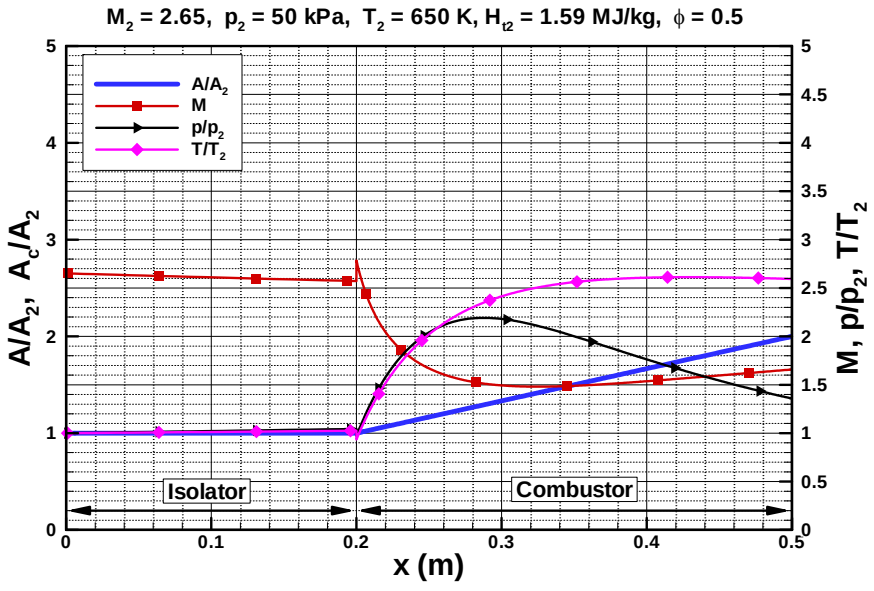

Figure 5: Fuelling at $\phi = 0.5$; attached flow through the isolator/combustor duct.

As the fuelling level is increased, the pressure rise in the duct can reach the point where flow separation can occur. In the current analysis the well known separation criterion of Korkegi[8] are used to determine if this occurs. When this does happen, an iterative technique is required to determine the axial position of separation, after which the core flow area is less than the geometric area until re-attachment occurs. It has

been found that in all instances there is a unique position for the separation point that allows the flow to re-attach smoothly in the divergent section. Furthermore, if the core flow reduces to subsonic conditions in the separated region, the flow re-attaches subsonically and then re-accelerates through a thermal throat at an axial position that can be calculated a priori, as outlined in Shapiro[6].

Figure 6 shows the calculated properties for a fuelling level of ϕ = 0.72. Here the pressure rise is high enough to separate the flow, and the analysis has been iterated to determine a separation point at x = 0.180 m. The core flow begins diffusing at this point at a rate dictated by eqn. 2, reaching a minimum area of A_c/A_2 = 0.822. Combustion of fuel acts to push the flow towards re-attachment, which occurs at x = 0.213 m (downstream of fuel injection) with M = 2.027. After re-attachment the Mach number continues to drop to a minimum of M = 1.087, and the pressure continues to rise to a maximum of P/P_2 = 3.51, after which the flow accelerates under the action of the increasing area to leave the combustor supersonically.

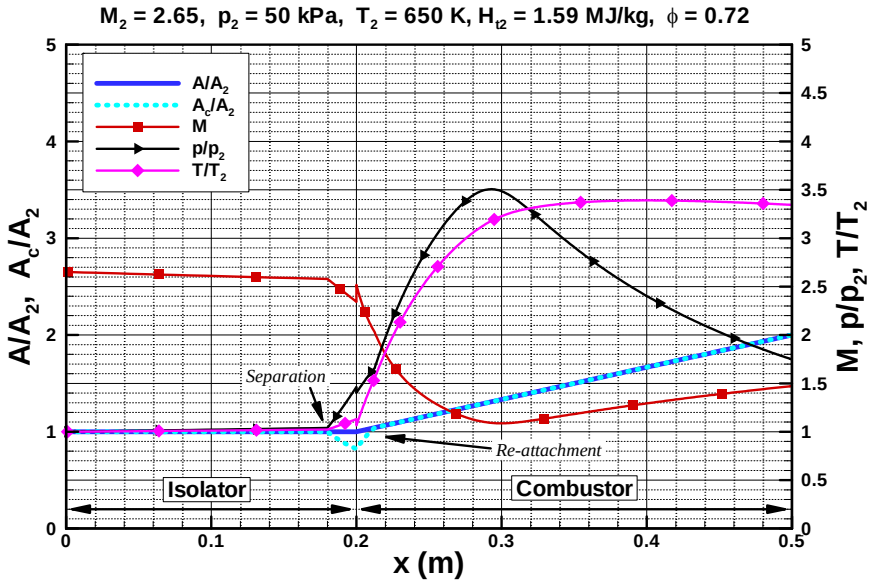

Figure 6: Fuelling at ϕ = 0.72; separated flow with a supersonic re-attachment.

Figure 7 shows the calculated properties for a fuelling level of ϕ = 0.81. Once again the pressure rise is high enough to separate the boundary layer, but in this instance the increased combustion has pushed the separation well upstream of fuel injection to x = 0.099 m. Furthermore, the Mach number of the core flow has dropped below Mach 1 to form what is known as a “thermal throat”. After separation the core flow reduces in area to a minimum of A_c/A_2 = 0.822 at the start of the combustor. The combustion then acts to push the core flow to re-attachment, and the Mach number drops through M = 1 with re-attachment at x = 0.284 with M = 0.960. The pressure also peaks at the point of re-attachment at P/P_2 = 4.24. The flow then re-accelerates through a thermal throat at x = 0.295 m and leaves the combustor supersonically. There is an important discussion in Shapiro[6] on the nature of a thermal throat and the manner in which attached flow can pass through the sonic point.

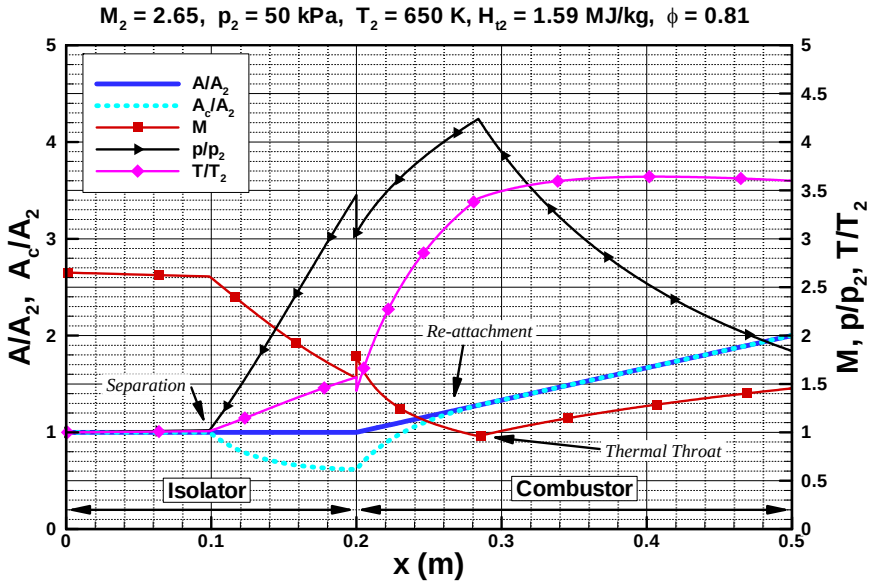

Figure 7: Fuelling at ϕ = 0.81; separated flow with a thermally throated.

A comparison of Figs. 5, 6 and 7 shows the upstream progress of the combustion influence with increasing heat release. For ϕ = 0.81, the separation is approximately half way along the isolator, and a designer would have to decide if extension of the isolator is justified to allow for increased combustion.

While it is recognized that this analysis involves the significant assumption of a perfect gas, it does however contain all the physical attributes that are exhibited by real flows. Similar analyses of combustion flows using finite volume techniques and equilibrium chemistry are presented by Auslender & Smart[9].

4.0 CONCLUDING REMARKS

The key feature of isolator design is the choice of the length required to "isolate" the inlet from influences propagating upstream from the combustor. Determination of this length requires modeling of separated, diffusing flows in internal ducts. The diffuser model of Ortwerth has been implemented here as part of a quasi-one-dimensional cycle code for the calculation of these flows. Given the distribution of heat release in the combustor and the isolator/combustor geometry, this code predicts the length of the upstream influence and hence the required isolator length.

5.0 REFERENCES

[1] Matsuo, K., Miyazato, Y. and Kim, H., 1999, "Shock train and pseudo-shock phenomena in internal gas flows", Progress in Aerospace Sciences, 35, p33-100.

[2] McLafferty, G.H., "Theoretical pressure recovery through a normal shock in a duct with initial boundary layer", Journal of the Aeronautical Sciences, Vol .20, No. 3, 1953, p169.

[3] Waltrup, P.J. and Billig, F.S., "Structure of shock waves in cylindrical ducts", AIAA journal, Vol .11, No. 10, 1973, pp 1404-1408.

[4] Ortwerth, P.J., 2001, "Scramjet Vehicle Integration", Scramjet Propulsion, Progress in Astronautics and Aeronautics, AIAA Washington DC, Chapter 17.

[5] Pandolfini, P.P., 1986, “Instructions for using ramjet performance analysis (RJPA) IBM-PC Version 1.0”, JHU-APL NASP-86-2.

[6] Shapiro, A.H., 1953, “The dynamics and thermodynamics of compressible fluid flow”, John Wiley & Sons, New York.

[7] Heiser, W.H. and Pratt, D.T., 1994, “Hypersonic Airbreathing Propulsion”, AIAA Education Series.

[8] Korkegi, R.H., 1975, “Comparison of shock induced two- and three-dimensional incipient turbulent separation”, AIAA Journal 13(4), p534-535.

[9] Auslender, A.H., and Smart, M.K., 2000, “Comparison of Ramjet Isolator Performance with Emphasis on Non-Constant Area Processes”, 2000 Joint Army-Navy-NASA-Air Force (JANNAF) Meeting, Monterey, California.